

Task No. 1

KINETICS OF ACETONE DESORPTION FROM POROUS SILICA MATERIALS

I. Task purpose

The purpose of this task is the estimation of kinetics of acetone desorption from porous silica to water using a spectrophotometric method.

II. Basic issues

1. Silica gel.
2. MCM-41.
3. UV-VIS spectrophotometry. Beer-Lambert law.
4. Kinetics of reactions. Integrated rate laws.

References

1. P. Atkins – “Physical Chemistry”, Oxford University Press, 1998.
2. P. Atkins, J. de Paula – “Physical Chemistry for the Life Sciences”, Oxford University Press, 2006.
3. K. Iler – “The colloid chemistry of silica and silicates”, Cornell University Press, Ithaca, New York, 1955.
4. Y. Wan, D. Zhao, Chemical Reviews, 107 (2006) 2821-2860.

Silicates are the oxides of silica, where the Si atom shows tetrahedral coordination, with four oxygen atoms surrounding the central Si atom – see Fig. 1.

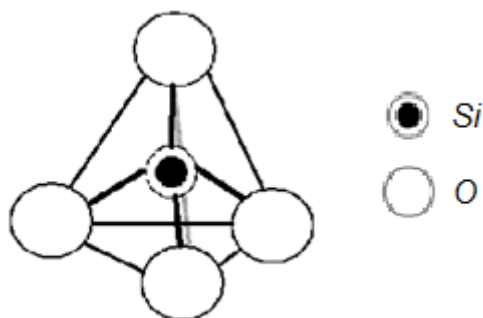


Fig. 1. Tetrahedral structural unit of silica.

In each of the thermodynamically stable forms of silica all oxygen atoms of the SiO_4 tetrahedra are shared with others, yielding the net chemical formula: SiO_2 . Silicon dioxide has a number of distinct crystalline forms (polymorphs, e.g. quartz, tridimite, cristobalite, faujasite, coesite, stishovite, moganite) in addition to the amorphous forms. Silica gels belong to amorphous silicates possessing non-recurrent network of tetrahedra, where all the oxygen corners connect two neighbouring tetrahedra. The amorphous structure of silica is shown in Fig. 2, where for clarity some oxygen atoms behind the plane of the picture or in front of it are omitted.

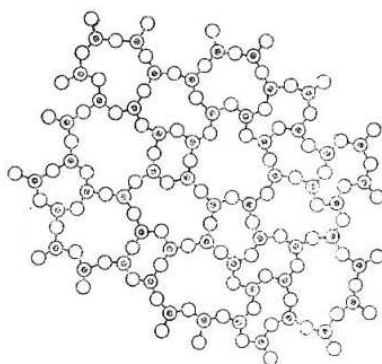


Fig. 2. The amorphous structure of silica gel [1].

Silica gel, a porous solid amorphous form of hydrous silicon dioxide, has the nominal chemical formula of $\text{SiO}_2 \cdot x\text{H}_2\text{O}$. It is constituted by randomly linked spheroidal polymerized silicate particles – the primary particles. The properties of silica gels are a result of the state of aggregation of the primary particles and the chemistry of their surfaces. The surface area, porosity and surface chemistry can be controlled during the production process.

Silica gels are fabricated in the sol-gel process as a result of polycondensation of orthosilicic acid:



This reaction leads to obtaining enlarged silicic acid macromolecules – by elongation, branching and cyclization of oxy-silicone chains. As a result, the silica particles covered by SiOH groups are obtained. The forms of created hydroxyl groups are collected in Fig. 3.

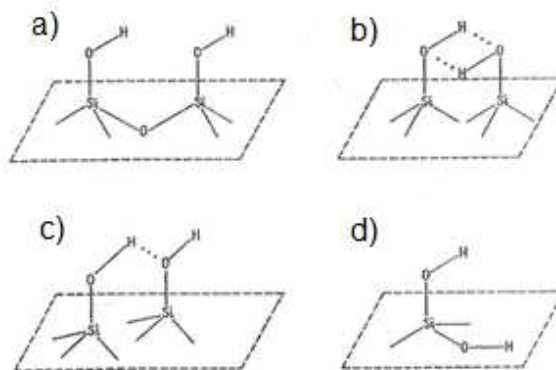


Fig. 3. Forms of hydroxyl groups on the surface of silica gel: a) single (isolated); b) hydrogen bonded; c) active; d) double (germinal) [1].

Structure characterization of amorphous silica gel Si-100 obtained using the low temperature nitrogen adsorption/desorption method is presented in Fig. 4 (a) and (b).

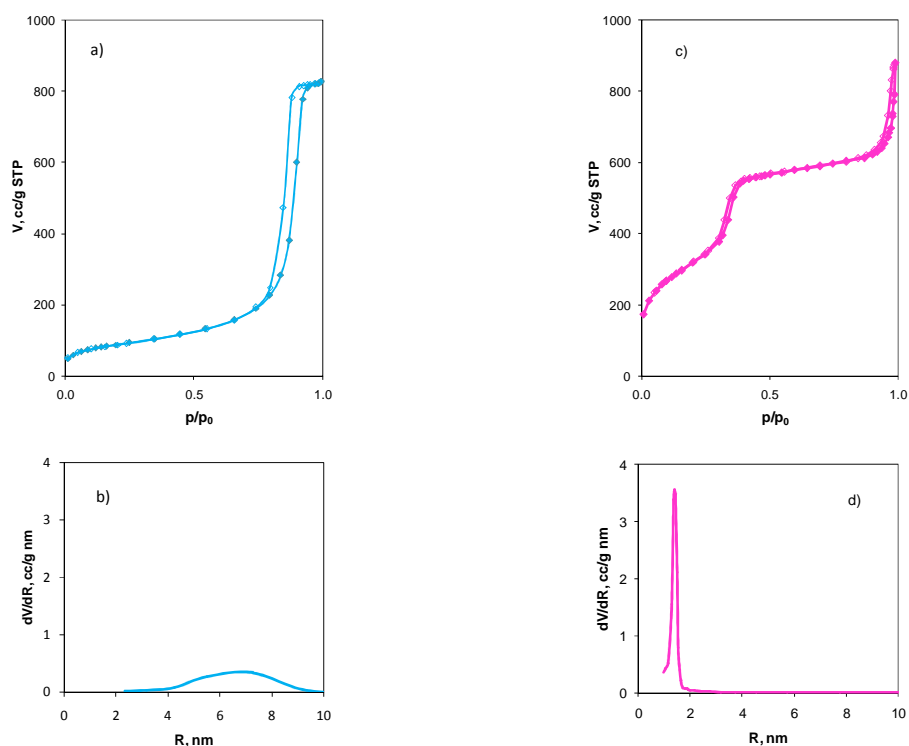


Fig. 4. Nitrogen adsorption/desorption isotherms (a, c) and pore size distributions (b, d) for Si-100 (a, b) and MCM-41 (c, d) samples.

Ordered mesoporous silica (OMS) materials are synthesized using a surfactant templating method (see Fig. 5). They present long-range ordered porous structures with narrow pore size distributions and large surface areas as well as pore volumes. Mobil Corporation research and development scientists for the first time reported the synthesis of novel ordered mesostructured materials known as MCM-41 family in 1992. These materials are characterized by regular arrays of uniform pores whose dimensions can be tailored through the choice of surfactant, additives and synthesis conditions. One of preparation theories is based on the formation of liquid crystals in mixtures of polar solvents and surfactants with non-polar tail group as follows: an increasing amount of surfactant molecules is dissolved in aqueous solution, and when the surfactant concentration reaches the critical micellar concentration (cmc), the surfactant molecules cluster together as micelles. These micelles are formed because the hydrophobic tails of the surfactant tend to agglomerate while their hydrophilic heads procure protection from water.

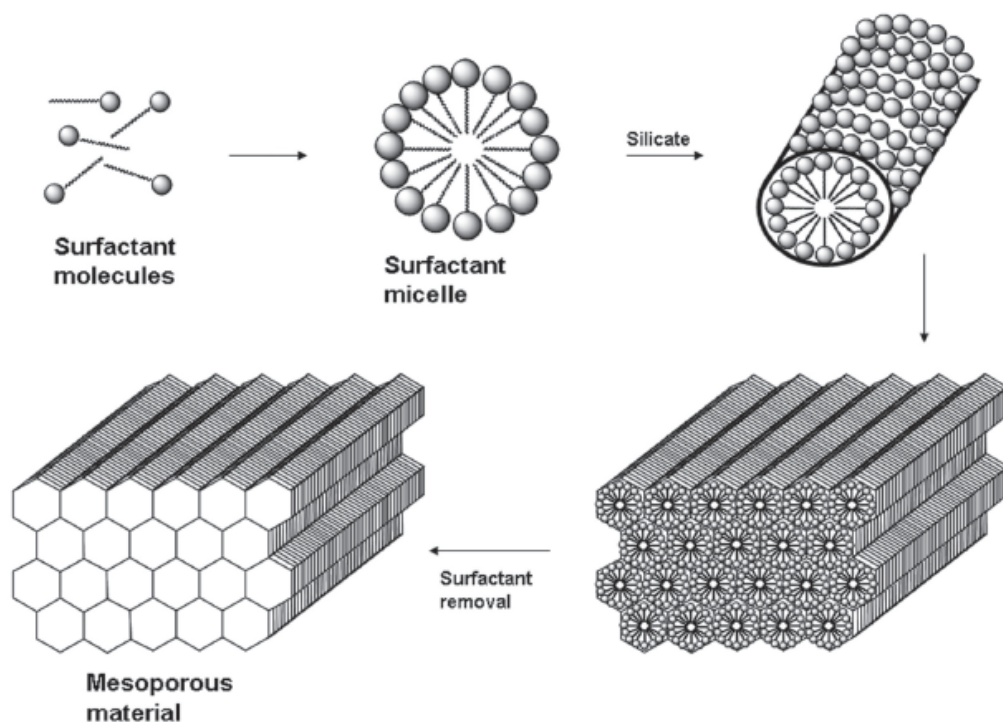


Fig. 5. Scheme of synthesis of ordered silica materials [2].

The final mesostructure of the material will depend on the organization of the surfactant molecules into the micellar liquid crystals which act as templates for the formation of the mesoporous materials. These liquid crystal structures depend on the composition and chemical nature of the surfactant and on the solution mixture conditions such as pH, temperature, surfactant concentration etc. The silica source has condensed around the micelles and the surfactant is removed by calcination (thermal degradation) or solvent

extraction. The molecular formulae of cationic surfactants used in preparation of ordered mesoporous materials are collected in Table 1.

Table 1. Molecular formulae of cationic surfactants [3].

Alkyltrimethyl quaternary ammonium surfactant	$\text{H}_3\text{C}-(\text{CH}_2)_{n-1}-\overset{\text{R}_1}{\underset{\text{R}_3}{\overset{\text{R}_2}{\text{N}}^+}}[\text{Br}^-] \quad \text{R}_1, \text{R}_2, \text{R}_3 = \text{CH}_3, \text{C}_2\text{H}_5, \text{C}_3\text{H}_7$ $n = 8 - 22$ $\text{H}_3\text{C}-(\text{CH}_2)_{n-1}-\overset{\text{CH}_3}{\underset{\text{CH}_3}{\overset{\text{CH}_3}{\text{N}}^+}}(\text{CH}_2)_{m-1}-\text{CH}_3[\text{Br}^-]$ $n = 8 - 22; m = 2 - 22$ $\text{H}_3\text{C}-(\text{CH}_2)_{n-1}-\overset{\text{CH}_3}{\underset{\text{CH}_3}{\overset{\text{CH}_3}{\text{N}}^+}}(\text{CH}_2)_m-\text{R}[\text{Br}^-] \quad \text{R} = \text{---} \langle \text{C}_6\text{H}_4 \rangle \text{---} \langle \text{C}_6\text{H}_4 \rangle \text{---} \text{OH}, \text{ etc}$ $n = 8 - 22; m = 0 - 3$
Gemini surfactant (C_{n-s-m})	$\text{H}_3\text{C}-(\text{CH}_2)_{n-1}-\overset{\text{H}_3\text{C}}{\underset{\text{H}_3\text{C}}{\overset{\text{H}_3\text{C}}{\text{N}}^+}}(\text{CH}_2)_s-\overset{\text{CH}_3}{\underset{\text{CH}_3}{\overset{\text{CH}_3}{\text{N}}^+}}(\text{CH}_2)_{m-1}-\text{CH}_3[2\text{Br}^-]$ $n = 8 - 22; s = 2 - 6; m = 1 - 22$
(C_{n-s-1})	$\text{H}_3\text{C}-(\text{CH}_2)_{n-1}-\overset{\text{H}_3\text{C}}{\underset{\text{H}_3\text{C}}{\overset{\text{H}_3\text{C}}{\text{N}}^+}}(\text{CH}_2)_s-\overset{\text{CH}_3}{\underset{\text{CH}_3}{\overset{\text{CH}_3}{\text{N}}^+}}(\text{CH}_3)[2\text{Br}^-]$ $n = 8 - 22; s = 2 - 6$
(18B ₄₋₃₋₁)	$\text{H}_3\text{C}-(\text{CH}_2)_{17}-\text{O}-\langle \text{C}_6\text{H}_4 \rangle-\text{O}-(\text{CH}_2)_4-\overset{\text{CH}_3}{\underset{\text{CH}_3}{\overset{\text{CH}_3}{\text{N}}^+}}(\text{CH}_2)_3-\overset{\text{CH}_3}{\underset{\text{CH}_3}{\overset{\text{CH}_3}{\text{N}}^+}}(\text{CH}_3)[2\text{Br}^-]$
Bolaform surfactant (R_n)	$\text{H}_3\text{C}-(\text{CH}_2)_n-\overset{\text{H}_3\text{C}}{\underset{\text{H}_3\text{C}}{\overset{\text{H}_3\text{C}}{\text{N}}^+}}(\text{CH}_2)_n-\text{O}-\langle \text{C}_6\text{H}_4 \rangle-\text{O}-(\text{CH}_2)_n-\overset{\text{CH}_3}{\underset{\text{CH}_3}{\overset{\text{CH}_3}{\text{N}}^+}}(\text{CH}_3)[2\text{Br}^-]$ $n = 4, 6, 8, 10, 12$
Tri-headgroup cationic surfactant ($\text{C}_{m-s-p-1}$)	$\text{H}_3\text{C}-(\text{CH}_2)_m-\overset{\text{H}_3\text{C}}{\underset{\text{H}_3\text{C}}{\overset{\text{H}_3\text{C}}{\text{N}}^+}}(\text{CH}_2)_s-\overset{\text{CH}_3}{\underset{\text{CH}_3}{\overset{\text{CH}_3}{\text{N}}^+}}(\text{CH}_2)_p-\overset{\text{CH}_3}{\underset{\text{CH}_3}{\overset{\text{CH}_3}{\text{N}}^+}}(\text{CH}_3)[3\text{Br}^-]$ $m = 14, 16, 18; s = 2; p = 3$
Tetra-headgroup rigid bolaform surfactant ($\text{C}_{n-m-m-n}$)	$\text{H}_3\text{C}-(\text{CH}_2)_n-\overset{\text{H}_3\text{C}}{\underset{\text{H}_3\text{C}}{\overset{\text{H}_3\text{C}}{\text{N}}^+}}(\text{CH}_2)_m-\overset{\text{CH}_3}{\underset{\text{CH}_3}{\overset{\text{CH}_3}{\text{N}}^+}}(\text{CH}_2)_m-\text{O}-\langle \text{C}_6\text{H}_4 \rangle-\text{O}-(\text{CH}_2)_m-\overset{\text{H}_3\text{C}}{\underset{\text{H}_3\text{C}}{\overset{\text{H}_3\text{C}}{\text{N}}^+}}(\text{CH}_2)_n-\overset{\text{CH}_3}{\underset{\text{CH}_3}{\overset{\text{CH}_3}{\text{N}}^+}}(\text{CH}_3)[4\text{Br}^-]$ $n = 2, 3, 4; m = 8, 10, 12$

This way prepared silica materials display exceptional properties: long-range ordering of the structure (see Figs 6 and 7), large surface area (usually over 1000 m²/g), large pore volume (ca 1 cm³/g) and uniform pore sizes (2-50 nm) – see Fig. 4 (c) and (d).

The conditions of reaction (pH, concentration of reagents) affect kind of the obtained materials (e.g. MCM-41, MCM-48, SBA-15) – see Fig. 8.

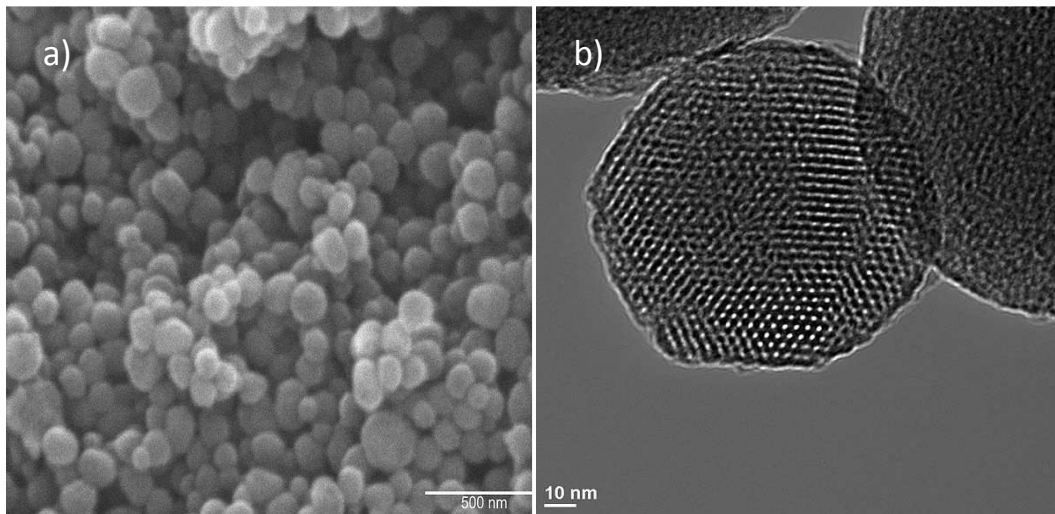


Fig. 6. Images of MCM-41 materials made using: a) scanning electron microscopy (SEM) [4]; b) transmission electron microscopy (TEM) methods [5].

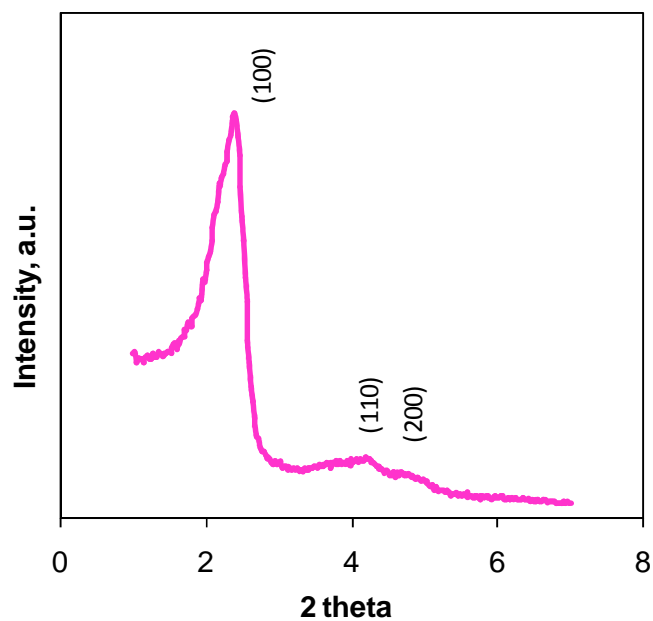


Fig. 7. X-ray diffraction patterns of MCM-41 material.

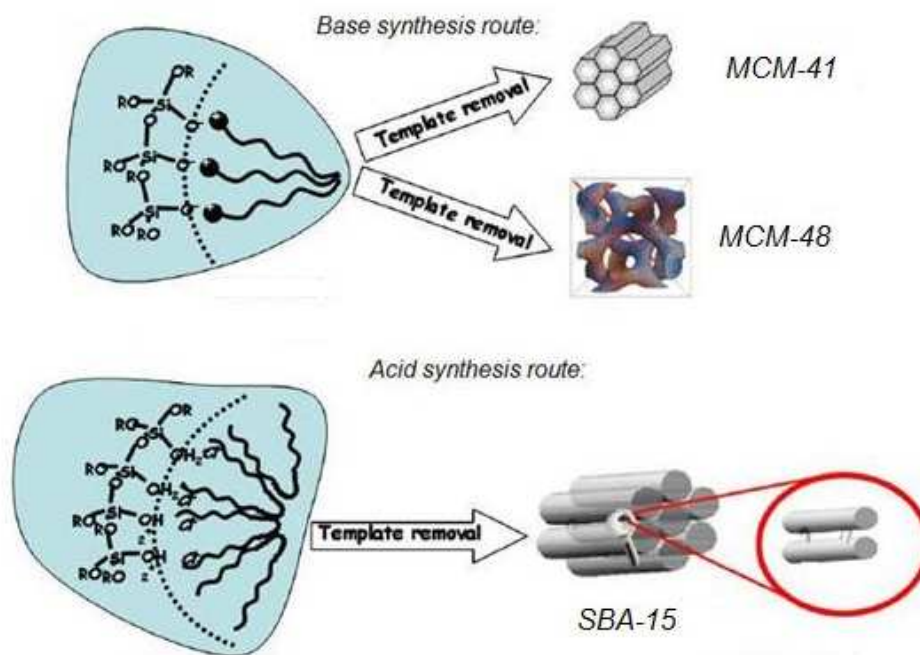


Fig. 8. Preparation routes of some mesoporous silica materials.

The ordered mesoporous silica materials offer the possibility of tuning the chemical properties of their surfaces to achieve the desired properties. The nanostructure, degree of organization and properties that can be obtained for such materials depend on the chemical nature of their components and the synergy between these components. The nature of the interface or the links and interactions exchanged by the organic and inorganic components has been used to categorize these hybrids into two main classes. Class I corresponds to all systems where no covalent or ion-covalent bonds are present between the organic and inorganic components. In such materials various components exchange only weak interactions (hydrogen bonding, van der Waals contacts, electrostatic forces). In class II materials a fraction of the organic and inorganic components is linked through strong chemical bonds (covalent, ion-covalent, or Lewis acid-base bonds).

The next important feature in tailoring hybrid networks concerns the chemical pathways that are used to design a given hybrid material. These chemical routes are schematically shown in Fig. 9. Path A corresponds to the conventional sol-gel chemistry. The hybrid network is obtained through the hydrolysis of organically modified metal alkoxides condensed with or without simple metallic alkoxides. This strategy yields amorphous hybrid materials, generally polydispersed in size and locally heterogeneous in chemical composition. For achieving the structure control at the nanoscopic level three main approaches can be conceived: self-assembled procedures

(route B in Fig. 9), assembly of well-defined nanobuilding blocks (NBBs) (route C) and combination of the two (route D).

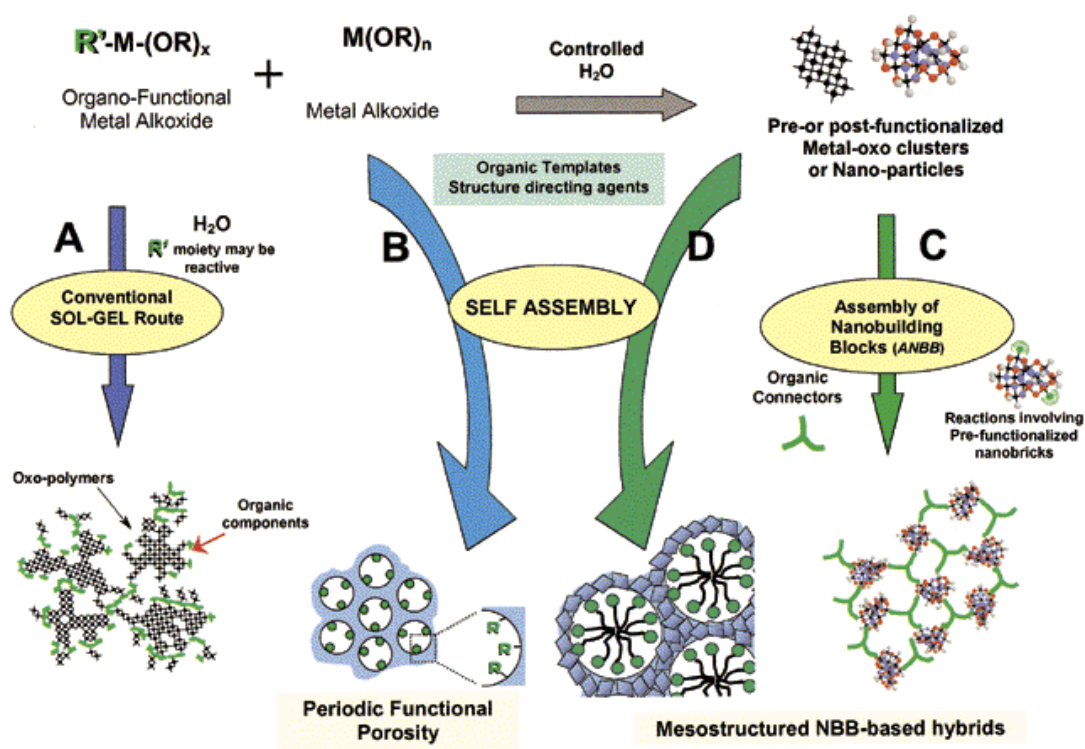


Fig. 9. Main paths for obtaining hybrid materials [6].

Routes B and D involve the use of organic structure-directing agents capable of self-assembly, giving rise to meso-organized phases. The hybrid interfaces can be here controlled and tuned and are very interesting because they demonstrate building a continuous range of organic polymers within the inorganic matrix. Route D represents strategy combining the nanobuilding block approach with the use of organic templates that self-assemble and allow controlling the assembly step. The NBBs units exhibit a large variety of interfaces between the organic and inorganic components (e.g. covalent bonding, electrostatic interactions). Depending on the set of chosen experimental conditions they will keep or lose their integrity. Therefore, they can be used as true building blocks that can be connected through organic spacers or surface-driven condensation reactions or as a reservoir of inorganic matter that can be delivered at the hybrid interface to build an extended inorganic network.

The functional groups which are usually introduced into the silica matrix are shown in Fig. 10. These groups can be incorporated during precipitation as is described above or by post-synthesis treatment and binding to silanol groups.

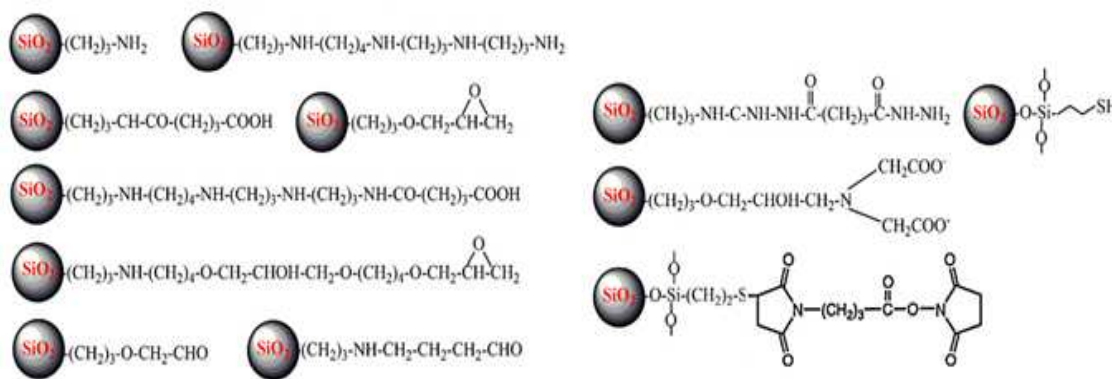


Fig. 10. Functional groups usually incorporated into the mesoporous silica matrix.

Spectrophotometry is the basis for a number of techniques used in chemical investigations. The key result for using the intensity of absorption at a particular wavelength to determine the concentration c of the absorbing species is the empirical *Beer-Lambert law*:

$$A = \varepsilon c l, \quad (1)$$

Where l is the length of the sample and the dimensionless absorbance, A , of the sample is given by:

$$A = \log(I_0/I), \quad (2)$$

Where I_0 and I are the incident and transmitted intensities, respectively – see Fig. 11. The quantity ε is called the molar absorption coefficient. It depends on the wavelength of the incident radiation and is greatest where the absorption is most intense. Typical values of ε for strong transitions are of the order 10^4 - 10^5 L mol⁻¹cm⁻¹.

It follows from the Beer-Lambert law that we can observe the appearance or depletion of a species during a reaction by monitoring changes in the absorbance of the reaction mixture.

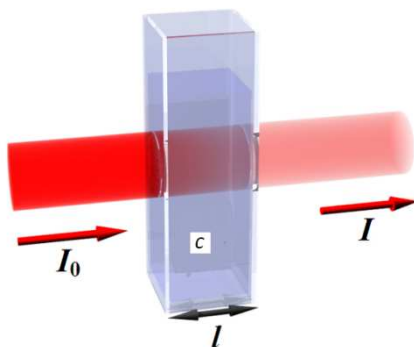


Fig. 11. Schematic representation of spectrophotometric measurements.

Spectrophotometers can work in the range of visible light and ultraviolet as well as near infra-red. The electromagnetic spectrum is shown in Fig. 12.

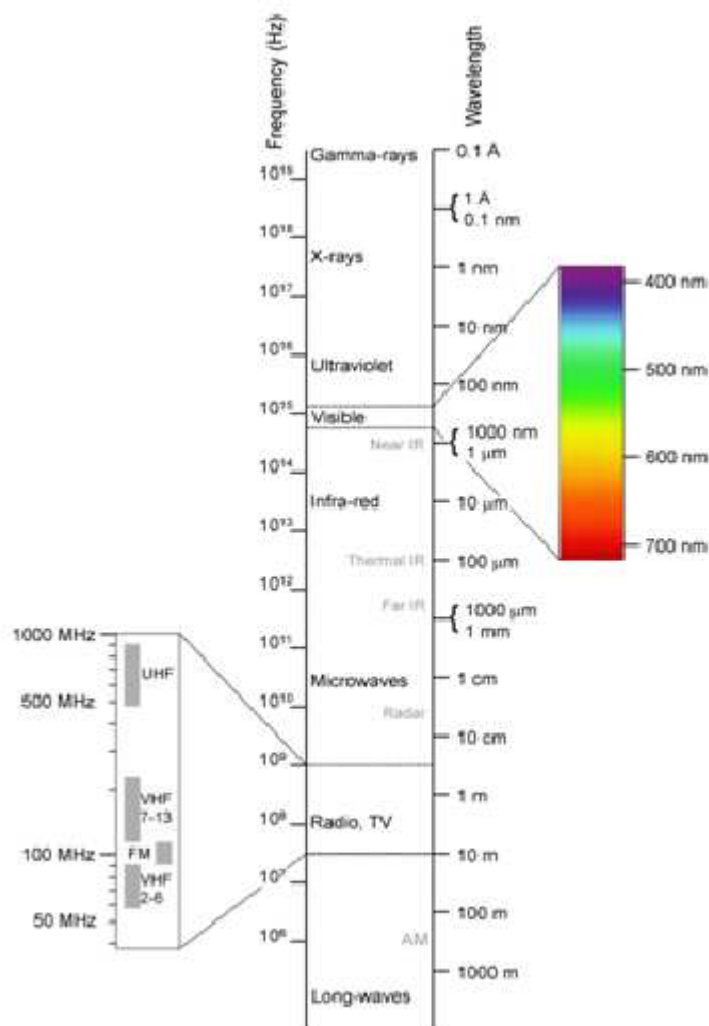


Fig. 12. Electromagnetic spectrum [7].

The rate of reaction is defined in terms of the rate of change the concentration of a designated species:

$$V = \pm \Delta c / \Delta t, \quad (3)$$

where Δc is the change in the molar concentration of the investigated species that occurs during the time Δt . An empirical observation is that the rate of reactions is often found to be proportional to the molar concentrations of the reactants raised to a simple power. The rate of reaction can be expressed as:

$$V = k [A]^m [B]^n. \quad (4)$$

[A] and [B] are the concentrations of the reactants A and B. The coefficient k , which is characteristic of the reaction being studied, is called the rate constant. It is independent

of the concentrations of the species taking part in the reaction but depends on the temperature. The m and n are not the respective stoichiometric coefficients of the balanced equation; they must be determined experimentally. An experimentally determined equation of this kind is called the rate law of the reaction.

Reactions can be classified on the basis of their order, the power to which the concentration of a species is raised in the rate law. A reaction with the rate law in equation (4) is m -order in A and n -order in B. The overall order of a reaction is the sum of the orders of all the components.

The rate equation is a differential equation and it can be integrated to obtain an integrated rate equation that links concentrations of reactants with time. If the concentration of one of the reactants remains constant (because it is catalyst or it is in great excess with respect to the other reactants), its concentration can be grouped with the rate constant, obtaining a *pseudo constant*; e.g. if B is the reactant whose concentration is constant, then the equation $V = k [A][B]$ can be written as $V = k'[A]$. The second order rate equation has been reduced to a *pseudo first order* rate equation. This makes the treatment to obtain an integrated rate equation much easier [8].

Table 2. Kinetic equations for zero-, first- and second-order reactions.

	Zero-order	First-order	Second-order
Rate law	$-\frac{d[A]}{dt} = k$	$-\frac{d[A]}{dt} = k [A]$	$-\frac{d[A]}{dt} = k [A]^2$
Integrated rate law	$[A] = [A]_0 - kt$	$[A] = [A]_0 e^{-kt}$	$\frac{1}{[A]} = \frac{1}{[A]_0} + kt$
Linear plot	$[A] \text{ vs. } t$	$\ln([A]) \text{ vs. } t$	$\frac{1}{[A]} \text{ vs. } t$

References

- [1] J. Ościk, “Adsorption”, Ellis Horwood Limited, Publishers – Chichester, 1979.
- [2] M. Colilla, M. Manzano, M. Vallet-Regi, International Journal of Nanomedicine, 3 (2008) 403-414.
- [3] Y. Wan, D. Zhao, Chemical Reviews, 107 (2006) 2821-2860.
- [4] http://en.wikipedia.org/wiki/File:Mesoporous_silica_SEM.jpg
- [5] http://en.wikipedia.org/wiki/File:Mesoporous_silica_closeup.jpg
- [6] C. Sanchez, G.J. de A.A. Soler-Illia, F. Ribot, T. Lalot, C.R. Mayer, V. Cabuil, Chemistry of Materials, 13 (2001) 3061-3083.
- [7] <http://en.wikipedia.org/wiki/File:Electromagnetic-Spectrum.png>
- [8] P. Atkins, J. de Paula – “Physical Chemistry for the Life Sciences”, Oxford University Press, 2006.

Experimental

A. Equipment and reagents

1. Instrumentation:

- Spectrophotometer CARY 100 Bio.

2. Equipment:

- 4 flasks (25 mL);
- Glass pipette (10 mL);
- 4 quartz cuvettes for the spectrophotometer.

3. Reagents:

- 3 samples of porous silica adsorbents (LiChroprep Si-60, MCM-41 and modified MCM-41) soaked in acetone and pressed into pellets;
- Initial water solution of acetone (10^{-2} M);
- Distilled water.

B. Task program

1. Calibration curve preparation.
2. Kinetics measurements.

C. Specifying the task performance

Measurements will be performed using a spectrophotometer CARY 100 Bio, shown in Fig. 13 - the instructions given by a teacher.



Fig. 13. Spectrophotometer CARY 100 Bio.

Calibration:

For preparation of the calibration curve, make a set of 4 solutions (concentrations are given in Table 2) by diluting the initial acetone in water solution (10^{-2} M) according to the previous calculations.

Measure the absorbance of each solution. Collect the obtained data in Table 1.

Table 1.

Flask	Concentration [mol/L]	Absorbance
1	10^{-3}	
2	$2,5 \cdot 10^{-3}$	
3	$5 \cdot 10^{-3}$	
4	$7,5 \cdot 10^{-3}$	

Measurements:

Put 0.05 g of silica sample (weighted with the accuracy to 2 mg) into a cuvette and add 3 ml of distilled water. Collect the amounts of components in Table 2:

Table 2.

Sample	Mass of adsorbent [g]	Mass of water [g]
Si-60		
MCM-41		
Mod. MCM-41		

After degassing the system, place the cuvette into a spectrophotometer and start collecting UV spectra (in accordance with the teacher's instruction) for 60 minutes every 3 minutes. Repeat this procedure for each adsorbent.

D. Analysis of results

Draw the calibration curve: plot of $A = f(c)$.

On the basis of the calibration curve calculate concentrations for each scan for subsequent samples at the wavelength 264 nm. Collect the results in Table 3.

Table 3.

Time [min]	Si-60		MCM-41		Mod. MCM-41	
	Absorbance	Concentration [mol/L]	Absorbance	Concentration [mol/L]	Absorbance	Concentration [mol/L]
3						
6						
9						
12						
...						

Draw plots of concentration vs time for the subsequent samples.

Convert each concentration from Table 3 into percent of acetone released following the calculations:

$$c = n/V = n \cdot d / m_{sol} \quad \rightarrow \quad n = c \cdot m_{sol} / d;$$

where: c – the concentration of acetone (from Table 3);

V – the volume of solution;

n – the number of moles;

d – the density of solution (for such dilute solution take $d = 1$ g/mL);

m_{sol} – the mass of the solution (practically equal to mass of water from Table 1).

$$m_A = n \cdot M_A;$$

where: m_A – the mass of acetone released to the solution;

M_A – the molar mass of acetone.

$$Rel = 100\% \cdot m_A / m_{A \max};$$

where: Rel – the percent of acetone release;

$m_{A \max}$ – the highest mass of acetone released from the given sample.

Collect the obtained results in Table 4.

Table 4.

Time [min]	Acetone release [%]		
	Si-60	MCM-41	Mod. MCM-41
3			
6			
9			
12			
...			

In one figure draw the plots of acetone released as a function of time for each sample.

Analyze the obtained results (taking into account the information about the modified MCM-41 sample given by a teacher) and draw conclusions concerning the kinetics of desorption of acetone from subsequent samples in water.